

# POST SCISSION NEUTRON EMISSION AND TRANSFORMATION OF FISSION FRAGMENTS YIELD: ARE THE REGULARITIES?

V.T. Maslyuk, O.O. Parlag, M.I. Romanyuk, O.I. Lengyel, O.M. Pop, N.I. Svatyuk

*Institute of Electron Physics, Universitetska str., 21, 88017 Uzhhorod, Ukraine*

*volodymyr.maslyuk@gmail.com*

## 1. Introduction

Studying the peculiarities of the formation of fission fragments and the processes of nuclear transformations of atomic nuclei is an important and urgent task of modern physics [1]. The success of its solution demonstrates the depth of our understanding of the fundamental issues of the stability of nuclear matter, the nature of nuclear forces, and nuclear transformations, for example, after the emission of post fission neutrons or beta particles. Applied aspects of this problem are:

- nuclear energy use;
- nuclear geophysics;
- radioecology;
- medicine with its advances in isotope and radiation therapies;
- a number of other applications.

Neutron activity is a permanent attribute of the fission of atomic nuclei and the related relaxation processes of the nuclear fragments' system with the emission of elementary nuclear particles [2]. Neutron emission spectra have their regularities connected to the topology of mass-charge spectra of fission fragments (MCSFF) with two or three humped yields curves. Thus, we are talking about “tooth-like” dependences of emitted neutrons  $n(A)$  on the mass ( $A$ ) or charge ( $Z$ ) of fission fragments, which follow the topology of the MCSFF nucleus [3]. To determine  $n(A)$  or  $n(Z)$  we need a qualitative experiment.

Investigation of the nature of the temporal evolution of MCSFF, for example, taking into account the post-fissile emission of elementary particles, is also a difficult task for theoretical research. The basis of modern theoretical approaches to describe the processes of nuclear fission and yields of fission fragments are various modifications of the liquid drop model. Within this model, it is possible to consider its spatial and deformation parameters and take into account the dynamics of atomic nuclei fission [4, 5]. The post-fission state of the nucleus is considered a bi-nuclide system in which nuclear transformations are neglected. Despite the significant progress made by these methods for nuclear physics, they all need some fitting parameters as the viscosity of nucleus, surface tension data on the density of states energy levels, etc.

The theoretical approach proposed in studied the post-scission ensemble of nuclei, created by all fission fragments with the thermodynamic parameters as temperature  $T$  and pressure  $P$ , are determined from the state of a fissile nucleus. This approach did not require fitting parameters and can study the fission characteristics both as light (pre actinides) and super-heavy nuclei. In this work, we present the results of the study of the influence of the emission of nuclear particles, mainly neutrons of fission, on the post-fission state of MCSFF, their isotopic and isobaric characteristics. These calculations are essential for understanding the nature of neutron activity and explaining the features of the dependences  $n(A)/n(Z)$  as, for

example, their “tooth-like” behavior. The calculation was performed on the example of actinide nuclei, the isotope  $^{235}\text{U}$ , for which there are sufficiently complete bases of nuclear physical constants.

## 2. Theory: the many ensembles model

The basics of the post-scission approach and the proposed statistical method for the systematization of fission fragments are described earlier [2, 6–9]. The study's subject is the post scission configurations or the ensemble of fission fragments of the fissioning nucleus with atomic mass  $A_0$  and the charge  $Z_0$  obtained due to thermodynamic ordering. This ensemble's single nuclear cluster, denoted by  $i$ , comprises two fission fragments  $j=1, 2$  with  $N_{p,j}^i$  protons and  $N_{n,j}^i$  neutrons when nuclear particles are emitted. Each cluster satisfies the following conservation conditions:

$$\begin{aligned} \sum_{j=1,2} (N_{p,j}^i + N_{n,j}^i + n_j^i) &= A_0, \\ \sum_{j=1,2} (N_{p,j}^i + m_j^i) &= Z_0; \end{aligned} \quad (1)$$

The positive sign  $m_j^i$  has the meaning of the number of emitted  $^+\beta$  and a negative one, respectively, the number of  $^-\beta$  particles. There are several options for constructing ensembles of fission fragments, taking into account post scission emission of nuclear particles. In the first one, such an ensemble can be built for fixed values of  $n, m$  in (1), i.e.  $n_1^i = n_2^i = n$ ,  $m_1^i = m_2^i = m$ . In this paper, considering the statistical nature of the emission of nuclear particles, we used an extended version, when  $\{n, m\}$  only sets the limits within which the emission of nuclear particles can occur. In other words, the ensemble will contain all the fission fragments obtained, taking into account both the neutron emission in the range  $(0 - n)$  and for beta particles, respectively, in the range  $(0 - m)$ . Only the conservation conditions (1) must be hold. By changing the sets  $\{n, m\}$ , it is possible to realize a different number of ensembles, each of which contains all the fission fragments obtained after emission of the nuclear particles within the range of values  $(0, 1, \dots, n)$  and  $(0, 1, \dots, m)$ . Further calculation in the case of many ensembles based on the following assumptions [10]:

- Nucleons with different binding energy for different nuclei fragments must be considered as statistically non-equivalents. This requires the introduction of new color statistics for systems whose energy is not additive in the number of particles;
- The most probable characteristics post fission ensembles of nucleus nucleons such as MCSFF, isotopic, isobaric outputs, characteristics of neutron activity are the observed values.

The proposed thermodynamic method contains no time variables and cannot consider the kinetics of the fission process. It is focused on investigating only the final state of the fission fragments ensemble realized after the complex radioactive-decay processes of neutron/beta particle emission both as prompt and delayed. However, the time evolution of MCSFF can be considered indirectly by constructing many nuclei ensembles resulting after the emission of chains of nuclear particles of different lengths. Increasing the size of the chains of emitted particles allows one to realize the state of the system of fission fragments after a long time since the scission of the initial nucleus. Such a procedure can simulate the

conditions for post-fission experiments when measurements are carried out after a long "cooling" time of an irradiated sample [10]. The parameters that determine the equilibrium condition for each of the investigated ensembles of nuclear fragments are subsequently deduced from the state of the minimum thermodynamic potential of constant pressure [11], which for  $i$ th nuclear cluster has the form:

$$G_i = \varepsilon_i - TS_i + PV_i \quad (2)$$

For  $i$ th cluster here  $\varepsilon_i$  is the internal energy, and  $V_i$ , respectively, the volume of a two fragments cluster,  $V_i = V_1^i + V_2^i$ . The  $\varepsilon_i$  values can be determined by the binding energy of the two-fragment cluster and have the negative values corresponding to the bound states of the nucleons. For different nuclear clusters, its spectrum  $\{\varepsilon_i\}$  is an additive quantity in the binding energy,  $B(N_{p,i}^j, N_{n,i}^j)$ , of the  $j$ th nucleus fragment from the  $i$ th cluster:

$$\varepsilon_i = \sum_{j=1,2} B(N_{p,i}^j, N_{n,i}^j). \quad (3)$$

Here according to (1),  $N_{n,1}^i + N_{n,2}^i = A_0 - n_1^i - n_2^i$ ,  $N_{p,1}^i + N_{p,2}^i = A_0 - m_1^i - m_2^i$ . Binding energies,  $B(N_{p,i}^j, N_{n,i}^j)$ , used in (3) are tabulated in [12,13], and their extrapolation is given, for example, in [14,15]. The term  $PV_i$  can be written as  $PN^i \Delta v$ , where  $N^i$  – number of fission-fragments nucleons,  $N^i = N_{n,1}^i + N_{n,2}^i + N_{p,1}^i + N_{p,2}^i$ , and  $\Delta v$  is the elementary volume of the nucleus per nucleon, which is 40–50 times larger than the size of the nucleon [1]. The constant  $P\Delta v$  is a parameter of the theory. It can be roughly evaluated through the ideal gas law:  $P\Delta V = \Delta N \cdot T$ , and  $\Delta N \sim 1$ , and the value of  $P\Delta v$  must be in the same order as  $T$ . More detailed value based on neutron emission spectra gives for  $P\Delta v$  range 3–5 MeV [2]. The configurational entropy  $S_i$  in (2):

$$S_i = \ln(\omega_i) \quad (4)$$

is calculated through the degeneracy factor  $\omega_i$  with the account of the statistical nonequivalence of nucleons with different specific binding energy:

$$\omega_i = A_0! / \left( \prod_{j=1,2} K(n_j^i) (N_{p,j}^i)! (N_{n,j}^i - n_j^i)! \right), \quad (5)$$

where  $n_j^i$  – number of fission neutrons of  $j$ th fission fragment from  $i$ th cluster,  $K(n_j^i) = 1/n_j^i!$ ,  $\prod_{j=1,2} x_j! = x_1! x_2!$ . From the (5), one can see that with increasing the nuclear temperature  $T$

entropy term in eq. (2) is responsible for the increase the symmetry of fission fragments yields. This is since the maximum  $\omega_i$  is achieved at  $N_{p,1}^i = N_{p,2}^i, N_{n,1}^i = N_{n,2}^i$ . Formulas (1) – (4) allow one to find the probability of realization or yield of two-fragments nuclear clusters of the  $i$ - sort. In the isothermal-isobaric ensemble, the probability of a microstate, here two-fragments cluster  $i$ , is defined by the term  $\exp(-G_i/T)$  [31] and has the form:

$$Y(N_{p,1}^i, N_{p,2}^i, N_{n,1}^i, N_{n,2}^i) = \omega_i \exp\{-(\varepsilon_i + PV_i)/T\} / z, \quad (6)$$

where  $\varepsilon_i$  is the spectrum values (3) of the two-fragments cluster,  $\omega_i$  determines its degeneration by the formula (5), the partition function of the system  $z$  is written as:

$$z = \sum_i \omega_i \exp\{-(\varepsilon_i + PV_i)/T\}. \quad (7)$$

The expression (6) refers to the probability of realization only of two-fragment clusters. The next step is calculating the distribution function  $F(A_1)/F(Z_1)$  for the single fission fragment with mass  $A_1$ , or charge  $Z_1$ . To construct them from the array of values, (6), one must select all the functions whose arguments satisfy the condition  $N_{p,1}^i + N_{n,1}^i = N_{p,2}^i + N_{n,2}^i = A_1$ . The summing of such functions and to spread this procedure for all  $A_1$  values is the next stage for mass spectrum finding. The same method is valid to build the charge spectra, only with selection for the argument  $N_{p,1}^i = N_{p,2}^i = Z_1$  from all the functions (6). The final stage is to apply the normalization procedure for the sums obtained and determine the normalized values of  $F(A_1)$  and  $F(Z_1)$ . These functions must satisfy the following equations:

$$\sum_{\langle A_1 \rangle} F(A_1) = \sum_{\langle Z_1 \rangle} F(Z_1) = 200\% \quad (8)$$

where the symbols  $\langle A_1 \rangle$ ,  $\langle Z_1 \rangle$  mean that the summation is over all masses/charges of heavy and light fission fragments.

### 3. The post fission emission of nuclear particles and the nuclear fission fragments yields: $^{235}\text{U}$

The studies were performed on the example of odd-even isotope  $^{235}\text{U}$ , whose MCSFF has been well established [16,17]. All possible schemes of post-fission emission of nuclear particles and construction of an array of many ensembles for them are considered. Each ensemble contains the  $^{235}\text{U}$  isotope fission fragments after the nuclear particles' emission within their length chains. For the  $j$ -th nucleus from the  $i$ -th cluster, the result of the emission of  $m_j^i$  beta particles leads to the transformation  $N_{p,j}^i \Rightarrow (N_{p,j}^i - m_j^i)$ , where the positive sign  $m_j^i$  is for  $+\beta$  and the negative for  $-\beta$  particles, respectively. After the emission of the neutrons  $n_j^i$ :  $N_{p,j}^i + N_{n,i}^i \Rightarrow N_{p,j}^i + N_{n,j}^i - n_1^i - n_2^i$ . The calculation carried out for the  $^{235}\text{U}$  shows that both the beta particles and the neutron's emission may change the most probable pairs of fission fragments' nucleon composition. It also favors the formation of most probable clusters with closed-shell fragments, having a greater specific binding energy. The neutrons emission leads to an increase in the configuration entropy (5) of the nuclear fission cluster. The most probable are two fragments fission clusters obtained from the minimum of the thermodynamic potentials of Gibbs (2) for a constant pressure ensemble. The results of calculations are given in Table 1 containing from  $M=1$  to five of the most probable two fragments clusters, both without and when taking into account the emission of nuclear particles.

The calculation was given in the "cold",  $T=0.5$  MeV and "hot"  $T=1.0$  MeV assumptions for the  $^{235}\text{U}$  fission temperature; the  $P\Delta v=3$  MeV. The sign in front of  $n$  is always positive, while the sign in front of  $m$  indicates the sort of beta particles emitted: minus suggests that there is the chain of  $\bar{\beta}$  particles from the  $(-m, 0)$  range; positive  $m$  values relate to  $^+\beta$  particles with their emission range  $(0, m)$ .

Table 1. The evolution of five the most probable two-fragment clusters after the  $^{235}\text{U}$  fission,  $M=1-5$ , after emission the neutrons of different chains' lengths:  $n$  defines all their sets from the ranges  $(0, n)$  and similar for beta-particles: the ranges  $(-m, 0)$  for  $-\beta$  particles  $(0, m)$  for  $+\beta$ , respectively.

$M$	$n=0; m=0$		$n=2; m=0$		$n=2; m=-2$	
	$T=0.5$ MeV	$T=1$ MeV	$T=0.5$ MeV	$T=1$ MeV	$T=0.5$ MeV	$T=1$ MeV
<b>1</b>	$\left\{ \begin{smallmatrix} 105 \\ 42 \end{smallmatrix} \text{Mo}, \begin{smallmatrix} 130 \\ 50 \end{smallmatrix} \text{Sn} \right\}$	$\left\{ \begin{smallmatrix} 105 \\ 42 \end{smallmatrix} \text{Mo}, \begin{smallmatrix} 130 \\ 50 \end{smallmatrix} \text{Sn} \right\}$	$\left\{ \begin{smallmatrix} 106 \\ 42 \end{smallmatrix} \text{Mo}, \begin{smallmatrix} 128 \\ 50 \end{smallmatrix} \text{Sn} \right\}$	$\left\{ \begin{smallmatrix} 103 \\ 42 \end{smallmatrix} \text{Mo}, \begin{smallmatrix} 128 \\ 50 \end{smallmatrix} \text{Sn} \right\}$	$\left\{ \begin{smallmatrix} 106 \\ 44 \end{smallmatrix} \text{Ru}, \begin{smallmatrix} 128 \\ 50 \end{smallmatrix} \text{Sn} \right\}$	$\left\{ \begin{smallmatrix} 107 \\ 44 \end{smallmatrix} \text{Ru}, \begin{smallmatrix} 124 \\ 50 \end{smallmatrix} \text{Sn} \right\}$
<b>2</b>	$\left\{ \begin{smallmatrix} 104 \\ 42 \end{smallmatrix} \text{Mo}, \begin{smallmatrix} 131 \\ 50 \end{smallmatrix} \text{Sn} \right\}$	$\left\{ \begin{smallmatrix} 104 \\ 42 \end{smallmatrix} \text{Mo}, \begin{smallmatrix} 130 \\ 50 \end{smallmatrix} \text{Sn} \right\}$	$\left\{ \begin{smallmatrix} 104 \\ 42 \end{smallmatrix} \text{Mo}, \begin{smallmatrix} 128 \\ 50 \end{smallmatrix} \text{Sn} \right\}$	$\left\{ \begin{smallmatrix} 101 \\ 42 \end{smallmatrix} \text{Mo}, \begin{smallmatrix} 130 \\ 50 \end{smallmatrix} \text{Sn} \right\}$	$\left\{ \begin{smallmatrix} 107 \\ 44 \end{smallmatrix} \text{Ru}, \begin{smallmatrix} 128 \\ 50 \end{smallmatrix} \text{Sn} \right\}$	$\left\{ \begin{smallmatrix} 106 \\ 44 \end{smallmatrix} \text{Ru}, \begin{smallmatrix} 125 \\ 50 \end{smallmatrix} \text{Sn} \right\}$
<b>3</b>	$\left\{ \begin{smallmatrix} 107 \\ 42 \end{smallmatrix} \text{Mo}, \begin{smallmatrix} 128 \\ 50 \end{smallmatrix} \text{Sn} \right\}$	$\left\{ \begin{smallmatrix} 107 \\ 42 \end{smallmatrix} \text{Mo}, \begin{smallmatrix} 128 \\ 50 \end{smallmatrix} \text{Sn} \right\}$	$\left\{ \begin{smallmatrix} 104 \\ 42 \end{smallmatrix} \text{Mo}, \begin{smallmatrix} 130 \\ 50 \end{smallmatrix} \text{Sn} \right\}$	$\left\{ \begin{smallmatrix} 97 \\ 40 \end{smallmatrix} \text{Zr}, \begin{smallmatrix} 134 \\ 52 \end{smallmatrix} \text{Te} \right\}$	$\left\{ \begin{smallmatrix} 106 \\ 44 \end{smallmatrix} \text{Ru}, \begin{smallmatrix} 126 \\ 50 \end{smallmatrix} \text{Sn} \right\}$	$\left\{ \begin{smallmatrix} 105 \\ 44 \end{smallmatrix} \text{Ru}, \begin{smallmatrix} 126 \\ 50 \end{smallmatrix} \text{Sn} \right\}$
<b>4</b>	$\left\{ \begin{smallmatrix} 103 \\ 41 \end{smallmatrix} \text{Nb}, \begin{smallmatrix} 132 \\ 51 \end{smallmatrix} \text{Sb} \right\}$	$\left\{ \begin{smallmatrix} 103 \\ 41 \end{smallmatrix} \text{Nb}, \begin{smallmatrix} 132 \\ 50 \end{smallmatrix} \text{Sn} \right\}$	$\left\{ \begin{smallmatrix} 102 \\ 42 \end{smallmatrix} \text{Mo}, \begin{smallmatrix} 130 \\ 50 \end{smallmatrix} \text{Sn} \right\}$	$\left\{ \begin{smallmatrix} 104 \\ 42 \end{smallmatrix} \text{Mo}, \begin{smallmatrix} 130 \\ 50 \end{smallmatrix} \text{Sn} \right\}$	$\left\{ \begin{smallmatrix} 105 \\ 44 \end{smallmatrix} \text{Ru}, \begin{smallmatrix} 127 \\ 50 \end{smallmatrix} \text{Sn} \right\}$	$\left\{ \begin{smallmatrix} 108 \\ 44 \end{smallmatrix} \text{Ru}, \begin{smallmatrix} 124 \\ 50 \end{smallmatrix} \text{Sn} \right\}$
<b>5</b>	$\left\{ \begin{smallmatrix} 102 \\ 40 \end{smallmatrix} \text{Zr}, \begin{smallmatrix} 133 \\ 52 \end{smallmatrix} \text{Te} \right\}$	$\left\{ \begin{smallmatrix} 112 \\ 44 \end{smallmatrix} \text{Ru}, \begin{smallmatrix} 123 \\ 48 \end{smallmatrix} \text{Cd} \right\}$	$\left\{ \begin{smallmatrix} 105 \\ 42 \end{smallmatrix} \text{Mo}, \begin{smallmatrix} 130 \\ 50 \end{smallmatrix} \text{Sn} \right\}$	$\left\{ \begin{smallmatrix} 102 \\ 40 \end{smallmatrix} \text{Mo}, \begin{smallmatrix} 129 \\ 50 \end{smallmatrix} \text{Sn} \right\}$	$\left\{ \begin{smallmatrix} 107 \\ 44 \end{smallmatrix} \text{Ru}, \begin{smallmatrix} 126 \\ 50 \end{smallmatrix} \text{Sn} \right\}$	$\left\{ \begin{smallmatrix} 114 \\ 46 \end{smallmatrix} \text{Pd}, \begin{smallmatrix} 118 \\ 48 \end{smallmatrix} \text{Cd} \right\}$

$M$	$n=3; m=0$	$n=3; m=-1$	$n=3; m=-2$	$n=3; m=-3$	$n=3; m=-4$
<b>1</b>	$\left\{ \begin{smallmatrix} 96 \\ 40 \end{smallmatrix} \text{Zr}, \begin{smallmatrix} 130 \\ 50 \end{smallmatrix} \text{Sn} \right\}$	$\left\{ \begin{smallmatrix} 105 \\ 43 \end{smallmatrix} \text{Te}, \begin{smallmatrix} 128 \\ 50 \end{smallmatrix} \text{Sn} \right\}$	$\left\{ \begin{smallmatrix} 106 \\ 44 \end{smallmatrix} \text{Ru}, \begin{smallmatrix} 128 \\ 50 \end{smallmatrix} \text{Sn} \right\}$	$\left\{ \begin{smallmatrix} 109 \\ 45 \end{smallmatrix} \text{Rh}, \begin{smallmatrix} 126 \\ 50 \end{smallmatrix} \text{Sn} \right\}$	$\left\{ \begin{smallmatrix} 112 \\ 46 \end{smallmatrix} \text{Pd}, \begin{smallmatrix} 122 \\ 50 \end{smallmatrix} \text{Sn} \right\}$
<b>2</b>	$\left\{ \begin{smallmatrix} 106 \\ 42 \end{smallmatrix} \text{Mo}, \begin{smallmatrix} 128 \\ 50 \end{smallmatrix} \text{Sn} \right\}$	$\left\{ \begin{smallmatrix} 103 \\ 43 \end{smallmatrix} \text{Te}, \begin{smallmatrix} 130 \\ 50 \end{smallmatrix} \text{Sn} \right\}$	$\left\{ \begin{smallmatrix} 108 \\ 44 \end{smallmatrix} \text{Ru}, \begin{smallmatrix} 126 \\ 50 \end{smallmatrix} \text{Sn} \right\}$	$\left\{ \begin{smallmatrix} 106 \\ 44 \end{smallmatrix} \text{Ru}, \begin{smallmatrix} 129 \\ 51 \end{smallmatrix} \text{Sb} \right\}$	$\left\{ \begin{smallmatrix} 110 \\ 46 \end{smallmatrix} \text{Pd}, \begin{smallmatrix} 124 \\ 50 \end{smallmatrix} \text{Sn} \right\}$
<b>3</b>	$\left\{ \begin{smallmatrix} 104 \\ 42 \end{smallmatrix} \text{Mo}, \begin{smallmatrix} 128 \\ 50 \end{smallmatrix} \text{Sn} \right\}$	$\left\{ \begin{smallmatrix} 102 \\ 42 \end{smallmatrix} \text{Mo}, \begin{smallmatrix} 131 \\ 51 \end{smallmatrix} \text{Sb} \right\}$	$\left\{ \begin{smallmatrix} 106 \\ 42 \end{smallmatrix} \text{Mo}, \begin{smallmatrix} 126 \\ 50 \end{smallmatrix} \text{Sn} \right\}$	$\left\{ \begin{smallmatrix} 112 \\ 46 \end{smallmatrix} \text{Pd}, \begin{smallmatrix} 121 \\ 49 \end{smallmatrix} \text{In} \right\}$	$\left\{ \begin{smallmatrix} 112 \\ 46 \end{smallmatrix} \text{Pd}, \begin{smallmatrix} 123 \\ 50 \end{smallmatrix} \text{Sn} \right\}$
<b>4</b>	$\left\{ \begin{smallmatrix} 104 \\ 42 \end{smallmatrix} \text{Mo}, \begin{smallmatrix} 130 \\ 50 \end{smallmatrix} \text{Sn} \right\}$	$\left\{ \begin{smallmatrix} 96 \\ 40 \end{smallmatrix} \text{Zr}, \begin{smallmatrix} 135 \\ 53 \end{smallmatrix} \text{J} \right\}$	$\left\{ \begin{smallmatrix} 109 \\ 44 \end{smallmatrix} \text{Ru}, \begin{smallmatrix} 126 \\ 50 \end{smallmatrix} \text{Sn} \right\}$	$\left\{ \begin{smallmatrix} 109 \\ 45 \end{smallmatrix} \text{Rh}, \begin{smallmatrix} 124 \\ 50 \end{smallmatrix} \text{Sn} \right\}$	$\left\{ \begin{smallmatrix} 111 \\ 46 \end{smallmatrix} \text{Pd}, \begin{smallmatrix} 124 \\ 50 \end{smallmatrix} \text{Sn} \right\}$
<b>5</b>	$\left\{ \begin{smallmatrix} 103 \\ 42 \end{smallmatrix} \text{Mo}, \begin{smallmatrix} 130 \\ 50 \end{smallmatrix} \text{Sn} \right\}$	$\left\{ \begin{smallmatrix} 106 \\ 43 \end{smallmatrix} \text{Te}, \begin{smallmatrix} 128 \\ 50 \end{smallmatrix} \text{Sn} \right\}$	$\left\{ \begin{smallmatrix} 106 \\ 44 \end{smallmatrix} \text{Ru}, \begin{smallmatrix} 126 \\ 50 \end{smallmatrix} \text{Sn} \right\}$	$\left\{ \begin{smallmatrix} 114 \\ 44 \end{smallmatrix} \text{Ru}, \begin{smallmatrix} 121 \\ 49 \end{smallmatrix} \text{In} \right\}$	$\left\{ \begin{smallmatrix} 118 \\ 48 \end{smallmatrix} \text{Cd}, \begin{smallmatrix} 118 \\ 48 \end{smallmatrix} \text{Cd} \right\}$

Figure 1 shows the results of the MCSFF calculations for the above cases. As one can see, the emission of  $^+\beta$  particles has almost no effect on their MCSFF compared to  $\bar{\beta}$  particles' emission. As mentioned above, it is because the asymmetric fission fragments of  $^{235}\text{U}$  are neutron-proficient nuclei. The emission of  $^+\beta$  particles only increases the neutron excess in the nucleus. The corresponding nuclear clusters don't increase the probability of realization than before the emission of  $^+\beta$  particles. Therefore, the effect of the emission of  $^+\beta$  particles on the formation of MCSFF is insignificant. When we consider the emission of  $-\beta$  particles, another nature of the MCSFF change will occur. In this case, there are significant changes in the MCSFF and the redistribution among the most probable fission fragments, see Tables 1. All this causes a change in the topology of the MCSFF. At  $n = 0$ , the peak of the light distribution fragments is formed by Mo isotopes. If one considers nuclear particles' emission, this peak mainly became would be created by the isotopes Mo, Nb, Zr, Ru, Pd and Cd. All these isotopes result from the influence of both the filled neutron shells  $N = 50$  and the entropy term (4), which stimulates the symmetry effects of the fission fragments.

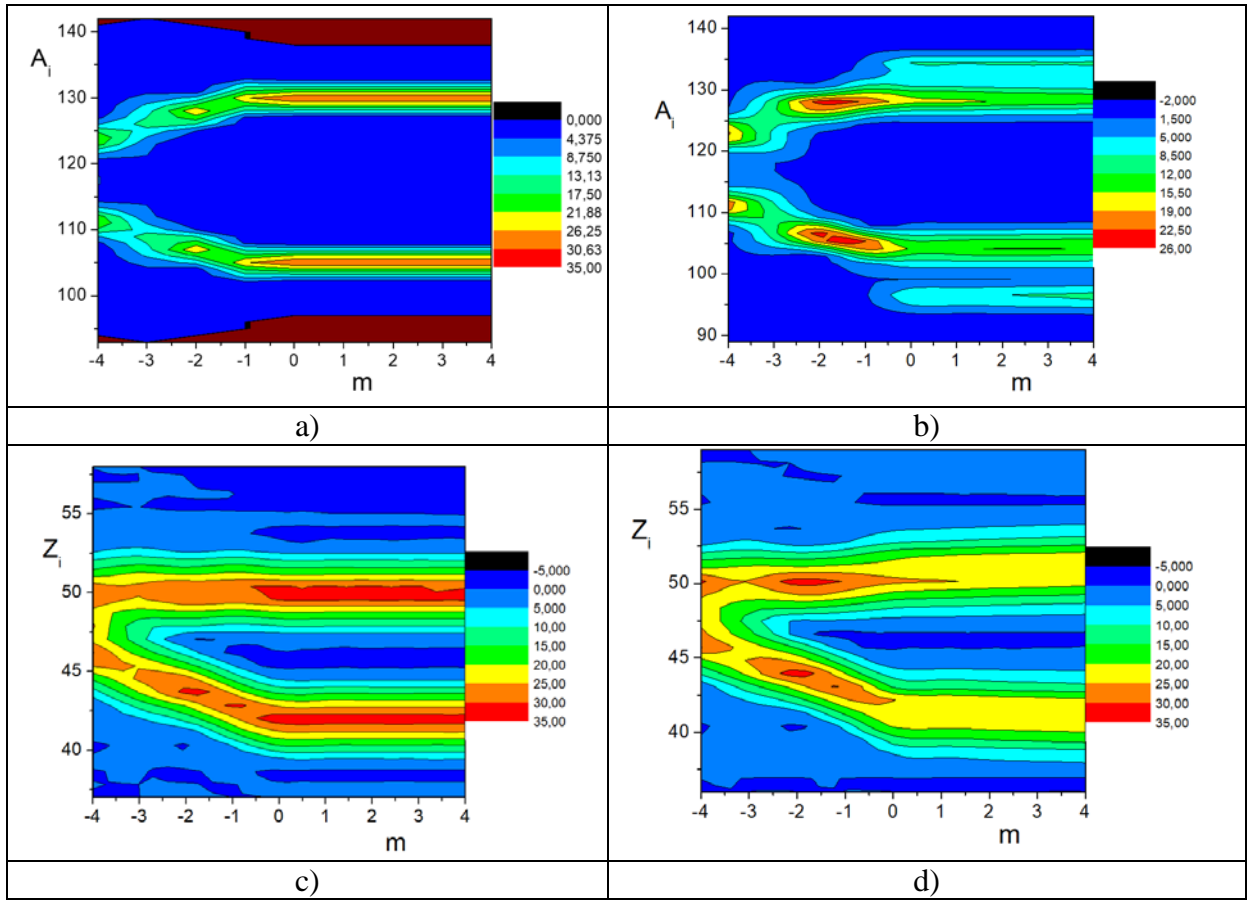


Fig. 1. The mass a), b) and charge c), d) fission fragments yields spectra of the  $^{235}\text{U}$  obtained with consideration the beta particles and the neutrons emission with different chains length. Here a) and c) were built for  $n=0$ ; b), d) with account the neutron emission chains with a capacity of  $n = 3$ . Minus in front of  $m$  suggests that there is the chain of  $\beta^-$  particles from the  $(-m, 0)$  range; positive  $m$  values relate to  $\beta^+$  particles with their emission range  $(0, m)$ .

For the peak of the heavy fission fragments, if we consider the neutron's emission, only the isotopes of Sn can be changing on the isotopes Sb, Te, Cd, J, In. These all neutron emissions lead to growing the configuration entropy of the nuclear clusters, affecting MCSFF symmetrization. Fig. 1 shows that nuclear particles' emission intensifies the convergence of the asymmetric peaks, which looks like enhanced the symmetry mode of the MCSFF yields. Herewith, the proportionality of two peaks shape for the light and heavy nuclei-fragments can be violated. This state is because the peak of heavy fission fragments within the magic number 50 is formed by the most massive amount of two fission fragment clusters than the corresponding light ones with  $Z$  from the range (41, 43). For mass spectra, the peak of heavy fission fragments near  $A = 132$  is the dominant one and formed by also the most massive sets of fragments closer to the doubly magic nuclei Sn. Genetically related light fission fragments sets have an  $A$  range (96 – 100).

It is very useful to investigate how the MCSFF transformation after the post-fission emission of nuclear particles affects the isotopic spectra and values of the probable value of  $Z_{\text{prob}}$  for a given  $A_i$ , or  $Z_{\text{prob}} = Z_{\text{prob}}(A_i)$ . In this work, the  $Z_{\text{prob}}$  calculations were performed using isotope spectra for each chemical element with a fixed  $Z$ . They have shown that all such

spectra are substantially varied, taking into account the post-fission emission of nuclear particles. Figure 2 (a) presents the results of such calculations for the Rb, Rh and Cs isotope spectra, all are a reliable markers of the fission of actinide nuclei. The sum of  $Y$  of the Rb, Rh, Cs isotopes yields were 100% normalized, and all data were fitted using B-spline procedure. This distribution was used to find value for  $Z_{\text{prob}}$ , considering the probable characteristics of the isotope spectra of these isotopes. The parameters for the beta particle and neutron chains were selected from Table 1. Fig. 2 b) demonstrates the dependence of  $Z_{\text{prob}}$  on the masses of the fission fragments  $A_i$  obtained with the same emission parameters as in Fig. 3 a). As one can see, the most significant changes of  $Z_{\text{prob}}$  from curve 1 to 2 occur for isotopes that do not contain magic numbers  $Z = 50, 82$ .

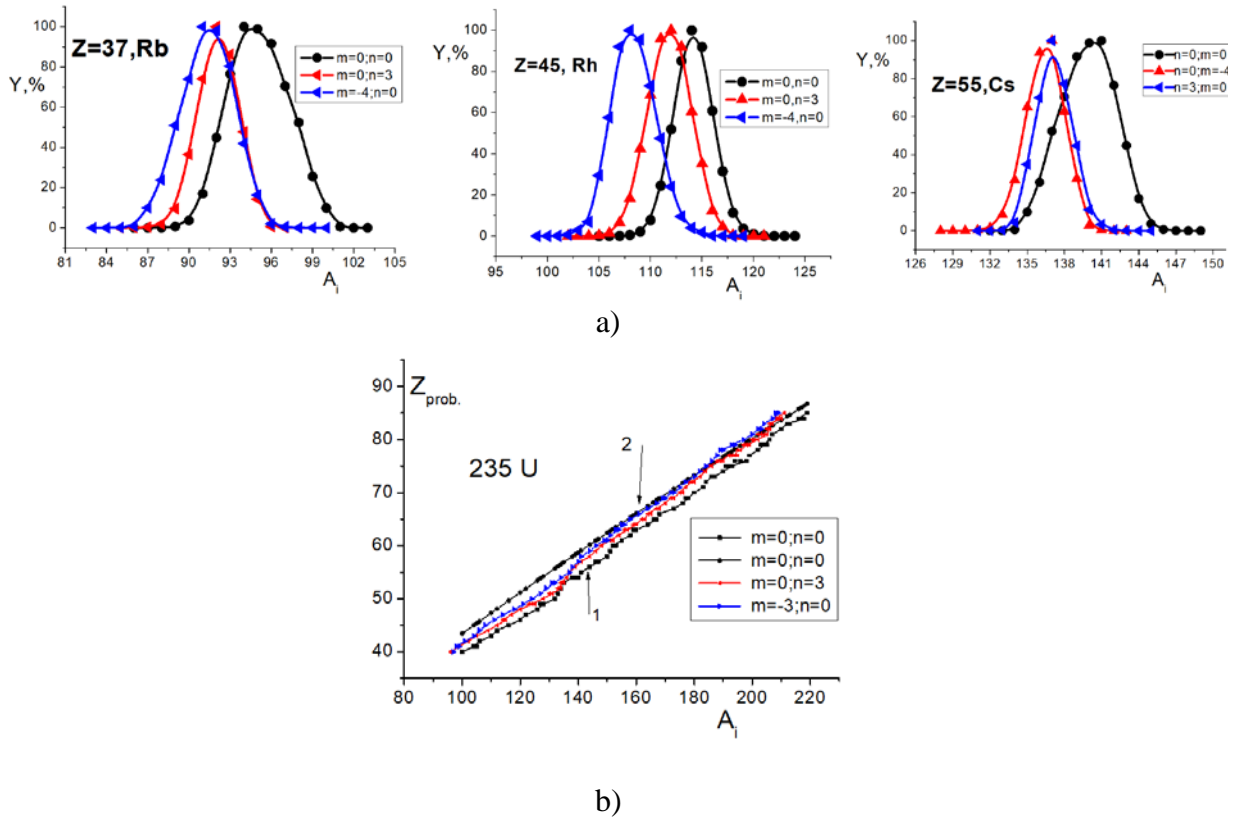


Fig. 2 (Color online) a) isotope spectra of Rb, Rh and Cs nuclides obtained without and accounting the post-scission emission of nuclear particles; b) dependencies between the masses  $A_i$  of fission fragments and their probable charges value  $Z_{\text{prob}}$ . Curve 1 is constructed for the pre-emission ( $m=n=0$ ) state of nuclear fragments, 2, respectively, is obtained from formula (9) as for beta-stable isobars. The curves for  $m = -3, n = 0$  and  $m = 0, n = 3$  illustrate how the emission of nuclear particles approaching  $Z_{\text{prob}}(A_i)$  curves to the beta-stable dependencies (9) .

The emission of nuclear particles shifts the dependences of  $Z_{\text{prob}} = Z_{\text{prob}}(A_i)$  from the values realized in the pre-emission case, ( $n=0, m=0$ ) and highlighted as 1, to dependence 2, determined from the liquid drop model for beta-stable isobars [1]:

$$Z_{ld} = \frac{A}{1.98 + 0.015A^{2/3}} \quad (9)$$

Moreover, such trends, Fig.2 b) are more pronounced, taking into account the emission of beta particles than neutrons or in the presence of neutrons and beta-particles.

#### 4. Method of many ensembles and function of neutron activity of nuclei: $^{236}\text{U}$

The proposed theoretical approach allows for the calculation of some observable neutron parameters: the total number of emitted neutrons as a function of the initial fragment mass (neutron emission function)  $\nu(A)$  and total neutron emission number  $\bar{n}$ . These functions are very important for neutron physics and numerous applications of neutron fluxes. Among the factors that determine  $\nu(A)$  and  $\bar{n}$ , the isotopic composition of the initial nucleus and its excitation energy or temperature  $T$  are the most important. The method of the  $\nu(A)$  function calculation is based on the probability determining of the two-fragment cluster's realization (yield) that contains a pre-neutron emission fragment with mass  $A$  and the equilibrium number of neutrons  $n$ . Considering that cumulative yield of the fission fragments,  $\bar{\nu}(A_i)$  is equal to value for all clusters containing the fragment with mass  $A_i$  from the cumulative chain:

$$\bar{\nu}(A_i) = 1/m \sum_{j=1}^m \nu_j(A_i), \quad (10)$$

where  $m$  is the length of the cumulative chain that forms the yields of the fragments with the mass  $A_i$ . The total number of neutrons emitted in the act of nucleus fission  $\bar{n}$  is calculated in a following way (normalization to 200% is used):

$$\bar{n} = 1/200 \sum_{A_i=1}^{A_i=A_0} \nu(A_i) F(A_i). \quad (11)$$

In Figure 3 the calculated and experimental [18] neutron emission functions for fission fragments of  $^{236}\text{U}$  are shown. The cumulative chain length was  $m=10$ . The values of  $T, P\nu_0$ , their fluctuation varies and the number of statistical events were the same as in the previous calculations described above. We obtained that the average value  $\bar{n}$  for such number of statistical events is 2.69 particles.

As one can see, the theoretical data agree well with the experiment. Moreover, the 9th order polynomial fit of obtained data (solid red line in Figure 3) reproduces the known experimental "saw-tooth"-curve of the neutron multiplicity, namely the peak about 115, minimum in vicinity of 128, the further growth in the range of 145 and decrease to 160. In addition, the proposed statistical method allows one to obtain the fine structure of  $\nu(A)$ , like local minima at 98, 104, 117, 121, 128, 134, 158 and local maxima at 92, 101, 109, 114, 119, 124, 133, 144, 154.



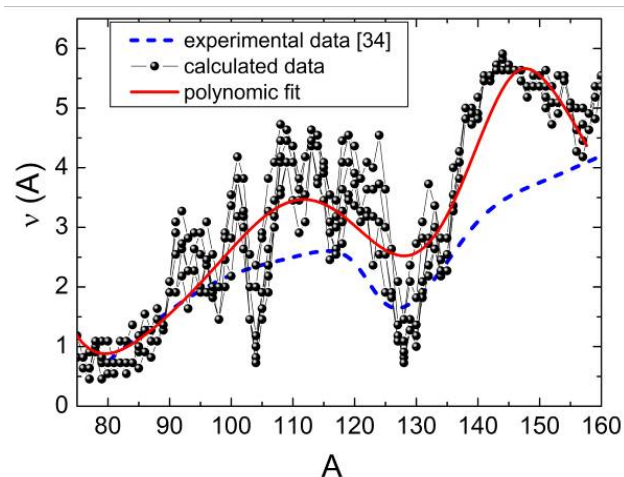


Figure 3. The fission neutron yield is given as a function of the fusion fragment mass of  $^{236}\text{U}$ : dashed line corresponds to the experimental data [18], circles with line present the calculated data and the solid line is the polynomial fit of our data (see more detail in the text).

It should be noted that the experimental dependences  $\nu(A_i)$  provide no data on such fine structure [3, 18, 20]. The fine structure might be caused by many factors such as presence of light and heavy fragments with the magic and near-magic numbers in the cluster; the optimal proton/neutron ratio in the fragments or influence of the odd/even effects, etc.

### Conclusions

Thus, the “many ensembles method” shows the possibility to investigate how the post-scission emission of the nuclear particles influences the MCSFF and establish the nature of the “saw-tooth” behavior curve of the neutron multiplicity. Note that the proposed theory assumes the same “saw-tooth” dependence for beta particles multiplicity. It is shown that the fission emission of nuclear particles of beta and neutrons is focused on the achievement of the state of beta-stable isobars by fragments of fission of the nuclear cluster (9). The calculation indicates that the neutron emission function  $n(A)$  must have a fine structure that is not obtained in the experiment. Note that it would be interesting to establish a similar experimental dependence of the beta particles emission function. Like neutrons, these particles contribute to the relaxation of fission fragments to the state of beta-stable isobars, described by the formula (9). The thermodynamic approach used in the paper allows us to establish the most probable two fragment clusters after the emission of nuclear particles and investigate their stability parameters. Such calculations help develop recommendations for processing nuclear experiments to study the fission fragments of atomic nuclei.

### References

1. V.Yu. Denisov, V.A. Plyuyko. Problems of nuclear physics and nuclear reactions: [https://inis.iaea.org/collection/NCLCollectionStore/ Public/45/091/45091761.pdf](https://inis.iaea.org/collection/NCLCollectionStore/Public/45/091/45091761.pdf).
2. V.T. Maslyuk et al, J. Mod. Phys., 1555–1562 (2013), 4. <http://dx.doi.org/10.4236/jmp.2013.412191>.
3. U. Brosa, Phys. Rev. C32 (1985) 1438–1441.

4. F.O. Ivanyuk et al., Phys. Rev. C. 054331, 1–10 (2018) 97.
5. M.D. Usang et al., Sci. Rep. 1525 1–9 (2019) 9.
6. V.T. Maslyuk et al., Phys. Part. Nucl. Lett. 4 (2007) 78.
7. V.T. Maslyuk et al., Nuclear Physics 955 (2016) 79.
8. V.T. Maslyuk et al., EPL, 112 (2015) 52001
9. V.T. Maslyuk et al., Phys. Rev. C 98 (2018) 064608.
10. V.T. Maslyuk et al. [arXiv:1907.04922v1](https://arxiv.org/abs/1907.04922v1) [nucl-th] .2019. 9 p.; Canad. J. Phys. (2021).  
<https://doi.org/10.1139/cjp-2020-356>
11. Zhirifalko. Statistical Physics of Materials (1973) 382 p. (in Russian).
12. Wang et al., Phys. Rev. C 84 (2011) 051303 (2011).
13. Wang et al., Chin. Phys. C36 (2012) 1603–2014.
14. G. Audi et al., Chin. Phys. C 41 (2017) 030001.
15. G. Audi et al., Chin. Phys. C 36 (2012) 1287.
16. R. Howell et al., Phys. Rev. C 100 (2019) 014608
17. M.E. Gooden et al., Nuclear Data Sheets 131, 319 (2016)
18. D.R. Nethaway et al., Phys. Rev. 139 (1965) 1505–1513.
19. Al-Adilia et al., Physics Procedia 47 (2013) 131–136.
20. M. Montoya, A. Rivera, Results in Physics 11 (2018) 449–451.